NASA MEMO 1-23-59A

NASA

MEMORANDUM

LOW-SPEED WIND-TUNNEL INVESTIGATION OF BLOWING BOUNDARY-LAYER CONTROL ON LEADING- AND TRAILING-EDGE FLAPS OF A LARGE-SCALE, LOW-ASPECT-RATIO, 45° SWEPT-WING AIRPLANE CONFIGURATION

By Ralph L. Maki

Ames Research Center
Moffett Field, Calif.

NATIONAL AERONAUTICS AND SPACE ADMINISTRATION
WASHINGTON
January 1959

NATIONAL AERONAUTICS AND SPACE ADMINISTRATION

MEMORANDUM 1-23-59A

LOW-SPEED WIND-TUNNEL INVESTIGATION OF BLOWING BOUNDARY-LAYER CONTROL ON LEADING- AND TRAILING-EDGE FLAPS OF A LARGE-SCALE, LOW-ASPECT-RATIO, 45° SWEPT-WING AIRPLANE CONFIGURATION

By Ralph L. Maki

SUMMARY

Blowing boundary-layer control was applied to the leading- and trailing-edge flaps of a 45° sweptback-wing complete model in a full-scale low-speed wind-tunnel study. The principal purpose of the study was to determine the effects of leading-edge flap deflection and boundary-layer control on maximum lift and longitudinal stability. Leading-edge flap deflection alone was sufficient to maintain static longitudinal stability without trailing-edge flaps. However, leading-edge flap blowing was required to maintain longitudinal stability by delaying leading-edge flow separation when trailing-edge flaps were deflected either with or without blowing. Partial-span leading-edge flaps deflected 60° with moderate blowing gave the major increase in maximum lift, although higher deflection and additional blowing gave some further increase. Inboard of 0.4 semispan leading-edge flap deflection could be reduced to 40° and/or blowing could be omitted with only small loss in maximum lift. Trailing-edge flap lift increments were increased by boundary-layer control for deflections greater than 45°. Maximum lift was not increased with deflected trailing-edge flaps with blowing.

INTRODUCTION

Boundary-layer control has been used to maintain theoretical lift effectiveness on highly deflected trailing-edge flaps. The usefulness of the large flap lift increments is often lost on thin swept-wing configurations where flow separation often occurs at the wing leading edge at relatively low angles of attack. Leading-edge stall control devices, such as slats and suction boundary-layer control applications, are successful in delaying this flow separation. However, in the belief

that blowing boundary-layer control is a more powerful method of stall control, studies are being made of its application in the delay of leading-edge air-flow separation.

The studies reported in references 1 and 2 show that blowing boundary-layer control at the knee of leading-edge flaps did suppress leading-edge stall and provided increases in maximum lift. The references indicate that the blowing flow requirements varied with angle of attack, and that lift and stability were sensitive to both spanwise variations of flap deflection and distribution of blowing. It seems likely that these variables must be tailored to each specific airplane configuration; therefore, similar tests on other configurations are required.

Flight studies of blowing boundary-layer control flaps on an F-100 airplane were planned at the Ames Research Center. It therefore seemed appropriate for the wind-tunnel program to include tests of a model with this wing plan form. This report presents the results of an investigation of a complete model with the wing and horizontal-tail geometry conforming to that of the F-100 airplane. Both leading-edge and trailing-edge flaps employed blowing boundary-layer control.

NOTATION

BLC boundary-layer control

b span

c chord, measured parallel to the plane of symmetry

$\bar{c}$ mean aerodynamic chord, $\dfrac{\int_0^{b/2} c^2 dy}{\int_0^{b/2} c\, dy}$

C_D drag coefficient

C_L lift coefficient

C_m pitching-moment coefficient referred to a point in the wing-chord plane at the longitudinal station of the wing panel $\bar{c}/4$ points

C_μ blowing flow coefficient, $\dfrac{WV_j}{gq_\infty S}$

g acceleration of gravity

q_∞ free-stream dynamic pressure

S area, excluding flap trailing-edge extension and including area blanketed by the fuselage

V_j velocity of ejected air at blowing nozzle exit

V_∞ free-stream velocity

W weight rate of flow from blowing nozzle

y spanwise distance from wing center line

α free-stream angle of attack, measured with respect to the wing-chord plane

δ deflection of flaps, measured normal to hinge line

Subscripts

f trailing edge

i inboard, 0.25 to 0.40 b/2

N leading edge

o outboard, 0.40 to 1.0 b/2

T wind-tunnel wall interference

t horizontal tail

max maximum

MODEL AND APPARATUS

The model used in this study is described in detail in table I and figure 1. The wing and horizontal tail simulate the F-100 airplane in plan form, section, and positioning. Figure 2 shows the model on the support struts in the wind-tunnel test section with trailing-edge and

full-span leading-edge flaps deflected. The wing was tested with the fuselage and vertical tail for all tests, and with the horizontal tail at 0° incidence for most tests; a few tests were made with the horizontal tail off.

The wing had 15-percent-chord plain leading-edge flaps extending from 0.25 to 1.0 semispan. For tests with constant deflection over this span length, they will be referred to as full-span leading-edge flaps. The flaps were divided at 0.40 semispan to allow different deflections inboard and outboard of this point. A blowing nozzle was located on the wing such that it became exposed when the leading-edge flap was deflected 30° (see fig. 3(a)). The nozzle gap was fixed by adjustable screws 2-1/2 inches apart along the nozzle lip. Nozzle heights of 0.015 and 0.03 inch (nominal values) were used during the tests.

A wing leading-edge modification was made which fit over the basic leading edge as a glove. It consisted of an increase in leading-edge radius added so as to camber the nose region with a minimum change to the wing upper surface (see fig. 3(b)). The gloves extended from 0.4 to 1.0 semispan (i.e., over the outboard flap).

The geometry of the trailing-edge flaps is described in table I and figures 1 and 3(c). The model wing planform conformed to the F-100 airplane geometry. The wing trailing edge was extended at the flap root section and the trailing-edge sweepback was reduced to meet the basic wing trailing edge at the wing-flap juncture. The flap and wing had continuous flat surfaces from the extended trailing edge forward to the lines of tangency with the basic wing surfaces. The flap blowing nozzle was located on the flap as shown in figure 3(c). The nozzle gap was continuous across the flap span with a nominal setting of 0.025 inch.

High-pressure blowing BLC air was supplied by two Westinghouse J-34 engines installed in the model fuselage. Bleed air was taken from the last stage of compression and piped to the wing leading-edge and trailing-edge regions. Cross sections of the wing ducts are illustrated in figures 3(a) and (c). Valves were installed in the fuselage piping to regulate the flow of air independently to the leading-edge inboard and outboard flaps and to the trailing-edge flaps. Total and static pressure taps (calibrated with standard ASME thin-plate orifices) and thermocouples in each air supply line were used to measure weight rates of air flow. Duct total pressure taps and thermocouples were distributed along the various flap ducts to allow computation of V_j (100-percent efficient jet expansion to free-stream static pressure was assumed).

TESTS AND CORRECTIONS

Lift, drag, and pitching-moment data were obtained at a free-stream dynamic pressure of 15 pounds per square foot. The Mach number was about 0.09 and the average Reynolds number was 8.2 million based on the wing mean aerodynamic chord. A list of the configurations tested is given in table II.

The data have been corrected for stream-angle inclination, wind-tunnel wall interference, and the interference of the support struts. The wall-interference corrections added were as follows:

$$\alpha_T = 0.95\ C_L$$

$$C_{D_T} = 0.017\ C_L^2$$

$$C_{m_T} = 0.012\ C_L \text{ (tail-on data)}$$

All coefficients are based on the model wing area (386 sq ft) without the flap trailing-edge extension.

Thrust of the jet engines was measured by tail-pipe total pressure readings which were calibrated at zero stream velocity. The effect of turning of the inlet air when the model was at angle of attack was computed. Thrust effects have been removed from the data.

RESULTS AND DISCUSSION

The model was tested with numerous combinations of leading- and trailing-edge flap deflections, with and without BLC, and with spanwise variations of leading-edge flap deflection and BLC. The complete longitudinal characteristics of only a selected group of test configurations will be discussed in detail. The effects on lift will be described for the numerous variations made in wing stall-control geometry and BLC. For these tests the longitudinal stability of the model was relatively insensitive to changes in spanwise distribution of leading-edge flap deflection and BLC.

General Effectiveness of Flaps and BLC

The characteristics in pitch of the model with various combinations of 60° leading-edge and 55° trailing-edge flap deflection, with and without BLC, are presented in figure 4. These data are representative generally of the effects of flap deflection and BLC on the model.

The C_{μ_N} value used with leading-edge flaps deflected in these data is above the value to which maximum lift increased rapidly with increasing C_{μ_N}; maximum lift increased slowly with further increase in leading-edge BLC. The C_{μ_f} value used with deflected trailing-edge flaps was sufficient to maintain essentially attached flow over the flaps. The effects of BLC variation will be discussed later.

Deflection of the leading-edge flaps without BLC increased lift at angles of attack above about 20° with trailing-edge flaps both undeflected and deflected. However, the effectiveness of the plain leading-edge flaps diminished rapidly above an angle of attack of about 12° when BLC was applied to the trailing-edge flaps. Application of blowing BLC to the leading-edge flaps greatly increased the leading-edge stall control with a large resulting increase in maximum lift with trailing-edge flaps both undeflected and deflected. Sizable lift increments due to trailing-edge flap deflection (with and without BLC) were retained to angles of attack above those normally encountered during approach to landing. The flap lift increment diminished at high angles, and $C_{L_{max}}$ was almost unaffected by flap deflection.

The rate of rise of drag coefficient for the wing with leading-edge flaps undeflected increased rapidly at lift coefficients above about 0.8. Without BLC, deflection of the leading-edge flaps increased the C_L for rapid C_D rise, but by rather small amounts. The high rate of rise started well below $C_{L_{max}}$ in all cases.

An increase in rate of C_D rise on thin swept wings is a sensitive indicator of the onset of flow separation near the wing leading edge. This flow separation generally originates near the wing tip region, and changes in pitching-moment curve slope often accompany the drag-coefficient increases. Because these changes indicate a decrease in static longitudinal stability, some wind-tunnel investigators have defined maximum usable C_L values by setting limits on change in dC_m/dC_L (ref. 1); rate of change of C_D rise can also be used. The reasoning is that if these changes in characteristics are sufficiently severe, $C_{L_{max}}$ may have no practical significance.

Flight investigations have been made attempting to define criteria which might successfully predict pilots' choices of landing-approach speeds. In reference 3, for example, drag effects were found to be a factor. A recent paper by Drinkwater, Cooper, and White (ref. 4), which treats the subject in detail from the pilot's point of view, shows the relative importance of maintaining positive static longitudinal stability and moderate rates of C_D rise in the complex of factors affecting choice of landing-approach speed. Pilots may consider an airplane "stalled" at a speed higher than actual stall speed by virtue of gradually deteriorating stability and control characteristics or increase in sink

rate with decreasing speed. However, flight analyses have not been able to define quantitative criteria for C_D or dC_m/dC_L. In wind-tunnel investigations of static longitudinal characteristics, the usability of the full lift range in flight may be indicated by a parabolic variation of C_D with C_L. The significance of such a variation is that it is the slowest theoretically possible increase in C_D with C_L and is associated with an absence of flow separation.

The increases in rate of C_D rise pointed out in figure 4 are quite pronounced at C_L values of about 0.8 to 0.9. Deflection of plain leading-edge flaps provided insufficient stall control to eliminate flow separation and the resulting limit on usable C_L. Application of BLC to the leading-edge flaps gave a parabolic rate of drag rise essentially to $C_{L_{max}}$, both with trailing-edge flaps undeflected and deflected. The parabolic curve included in figure 4(b) helps illustrate the small degree of departure from a potential-flow drag variation for the case with leading-edge flaps deflected with BLC. Leading-edge BLC, then, both increased $C_{L_{max}}$ and eliminated evidence of any serious flow separation up to $C_{L_{max}}$. This result was true for most leading-edge BLC configurations tested, so little attention will be given to drag characteristics in the later discussion of results with other variations in wing geometry.

The values of drag at low angles of attack with trailing-edge flaps deflected and BLC on (fig. 4(b)) are inconsistent. A review of the drag data for all configurations tested indicate the drag with leading- and trailing-edge flaps deflected with BLC only on the trailing-edge flaps (fig. 4(b)) to be abnormally low; no reason could be found for this.

The plain wing (all flaps undeflected) exhibited longitudinal instability through a range of lift coefficients starting at about the C_L at which the high rate of drag rise initiated (C_L about 0.8). Deflection of the leading-edge flaps without BLC eliminated the unstable moment variations; however, the instability persisted with trailing-edge flaps deflected. This instability, combined with the simultaneous increase in rate of C_D rise already noted would most likely limit the usable C_L in flight at this point. With BLC applied to the leading-edge flaps, the instability was eliminated for all trailing-edge flap conditions; the moment variations were essentially linear to $C_{L_{max}}$.

Horizontal-Tail Contribution to Stability

Instability in pitch of swept wings at moderate lifts is associated with stall at the wing tip region. However, complete-model characteristics are critically dependent on horizontal-tail volume and vertical position. The low tail placement on this model gave the stable tail contribution required for satisfactory moment variation for a wide variety of deflected

leading-edge configurations. The tail contribution to stability is shown in figure 5 for three wing configurations. The complete-model characteristics for two of these configurations have been presented in figure 4 and discussed ($\delta_N = 0^\circ$ and 60° full span). The third has nonuniform spanwise leading-edge deflection. It will be shown later in the discussion that this configuration provides a high $C_{L_{max}}$ with minimum BLC. Because of the large favorable tail contribution to stability, the complete-model pitching-moment characteristics were relatively insensitive to spanwise changes in deflection and distribution of BLC. This is in contrast to the results reported in reference 1 on tests of a high-tail model (also 45° wing sweepback) in which careful tailoring of span distribution of leading-edge flap deflection and BLC was required for satisfactory stability in pitch. Test results reported in reference 2 on a 49° swept-wing model are intermediate to those of reference 1 and this study; with a tail in the extended wing-chord plane, pitching-moment variations were insensitive to span distribution of leading-edge blowing BLC, but the tail contribution to stability was insufficient to eliminate all evidence of pitch-up.

Effects on Maximum Lift of Changes in Leading-Edge Configuration

The effects of leading-edge flap deflection with various BLC arrangements on maximum lift are shown in figure 6. Maximum lift increases almost linearly with full-span deflection up to 60° with moderate BLC (fig. 6(a)). The data with higher C_{μ_N} values show increased $C_{L_{max}}$ to 70° deflection. It is believed that an increase would have resulted with moderate C_{μ_N} at 70° deflection. For example, the data point in figure 6(b) for $\delta_{N_i} = 60^\circ$, $\delta_{N_o} = 70^\circ$, $C_{\mu_N} = 0.036$ is at $C_{L_{max}} = 1.93$; this is somewhat above the extrapolated curve in figure 6(a) for moderate C_{μ_N} and 70° deflection full span.

Effects of changes in spanwise distribution of leading-edge flap deflection with full-span and partial-span BLC are shown in figure 6(b). With the outboard flaps (0.4 to 1.0 semispan) deflected 60°, the inboard deflection can be reduced to 40° and BLC omitted with little loss in maximum lift. With 70° deflection outboard, the inboard deflection must be at least 60° to avoid a significant loss in $C_{L_{max}}$. The leading-edge outboard contour change (camber and radius increase) provided a lift increase equivalent to about 10° added flap deflection. These data show that very high values of $C_{L_{max}}$ are possible if sufficient bleed air for BLC is available, and if very high nose flap deflections are used. The configuration with $\delta_{N_i} = 40^\circ$, $\delta_{N_o} = 60^\circ$, and $C_{\mu_{N_o}} = 0.015$ appears to be a practical compromise between the attainment of high $C_{L_{max}}$ and economy of BLC.

The variation of $C_{L_{max}}$ with C_{μ_N} is shown in figure 7. Large increases in maximum lift are obtained with moderate values of C_{μ_N} full span. Maximum usable C_L values are shown for $C_{\mu_N} = 0.005$ and 0.010 because sharp reductions in lift-curve slope and increases in rate of C_D rise occurred at these C_L values, although lift did continue to increase at higher angles of attack. The meager partial-span BLC data appear generally to agree with the full-span BLC results. Little further benefit accrues from increasing C_{μ_N} values above about 0.03. Differences in $C_{L_{max}}$ with and without BLC over the inboard region (0.25 to 0.40 semispan) are shown in figure 6 for several combinations of leading-edge flap deflection. The increment in $C_{L_{max}}$ due to inboard BLC is 0.06 or less with $\delta_{N_o} = 60^o$, but is more than 0.15 with $\delta_{N_o} = 70^o$.

The trends of $C_{L_{max}}$ noted above with changes in distribution of δ_N and C_{μ_N} are similar to those reported in reference 1.

Trailing-Edge Flap Lift Effectiveness

Lift data with several trailing-edge flap deflections are given in figure 8. Maximum lift varies only slightly with δ_f, with or without BLC. With $\delta_f = 45^o$, the flow is essentially attached without BLC; hence, no lift increment due to blowing was measured at 0^o angle of attack. Flap lift increment at low angles of attack is reduced about 0.2 with the horizontal tail as a result of increased downwash at the tail. Lift per unit flap deflection reduces at deflections above 45^o even with C_{μ_f} somewhat above that required for apparent flow attachment.

Blowing Flow Requirements

Variations of C_L with C_{μ_N} full span and partial span at several angles of attack are shown in figure 9. The value of C_{μ_N} required for attached flow (above which C_L increases more slowly with increase in C_{μ_N}) increases with increasing α. A change in blowing nozzle height, or gap, made no material difference in the results. This again supports the use of C_{μ_N} as a correlating parameter for BLC requirements (when $V_j/V_\infty \gg 1$).

Variations of C_L with C_{μ_f} for several trailing-edge flap deflections are shown in figure 10. With 45^o deflection no lift increment due to BLC was measured (as noted previously in the discussion of fig. 8). Even for 65^o flap deflection the value of C_{μ_f} required for the major increase in C_L is small.

CONCLUDING REMARKS

The results of this study showed that blowing BLC at the knee of leading-edge flaps was effective in delaying air-flow separation at the wing leading edge. Leading-edge flap deflection alone was sufficient to maintain static longitudinal stability with trailing-edge flaps undeflected. Leading-edge flap blowing was required to maintain longitudinal stability by delaying leading-edge flow separation when trailing-edge flaps were deflected with or without BLC. Leading-edge flap deflection of 60° from 0.4 to 1.0 semispan with $C_{\mu N}$ = 0.015 to 0.03 over this region gave the major improvements in $C_{L_{max}}$, although higher deflections and additional blowing did give further benefit. Inboard of 0.4 semispan leading-edge flap deflection could be reduced to 40° and/or blowing could be omitted with only small loss in $C_{L_{max}}$.

Trailing-edge flap lift increments were increased by BLC for deflections greater than 45°. Without leading-edge deflection, flap lift was lost at moderate angles of attack and $C_{L_{max}}$ was reduced with increasing flap deflection. With adequate leading-edge flap deflection and BLC, sizable flap lift increments were retained to angles of attack above those normally encountered in the landing-approach condition.

The low horizontal tail used on the model had a large favorable effect on the static longitudinal stability of the complete model.

Ames Research Center
National Aeronautics and Space Administration
Moffett Field, Calif., Oct. 22, 1958

REFERENCES

1. Hickey, David H., and Aoyagi, Kiyoshi: Large-Scale Wind-Tunnel Tests of an Airplane Model With a 45° Sweptback Wing of Aspect Ratio 2.8 Employing High-Velocity Blowing Over the Leading- and Trailing-Edge Flaps. NACA RM A58A09, 1958.

2. Fink, Marvin P., and McLemore, H. Clyde: High-Pressure Blowing Over Flap and Wing Leading Edge of a Thin Large-Scale 49° Swept Wing-Body-Tail Configuration in Combination with a Drooped Nose and a Nose with a Radius Increase. NACA RM L57D23, 1957.

3. Lean, B., and Eaton, R.: The Influence of Drag Characteristics on the Choice of Landing Approach Speeds. R.A.E. TN Aero 2503, April 1957.

4. Drinkwater, Fred J., III, Cooper, George E., and White, Maurice D.: An Evaluation of the Factors Which Influence the Selection of Landing Approach Speeds. Paper presented to Flight-Test Panel of the Advisory Group for Aeronautical Research and Development (AGARD), Copenhagen, Denmark, Oct. 20-24, 1958.

TABLE I.- GEOMETRIC DATA FOR THE MODEL

Wing	
Area excluding flap trailing-edge extension, sq ft	386.0
Span, ft	38.6
Aspect ratio	3.86
Taper ratio	0.26
Mean aerodynamic chord, ft	11.17
Sweepback of the quarter-chord line, deg	45
Dihedral angle, deg	0
Basic airfoil section, streamwise, constant	NACA 64A007
Leading-edge flap	
Chord in percent of local wing chord, c, constant	15
Inboard flap extent, percent semispan, measured at hinge	25 to 40
Outboard flap extent, percent semispan, measured at hinge	40 to 100
Trailing-edge flap	
Chord, measured streamwise from hinge to trailing edge, ft	
Inboard end (0.151 semispan)	3.93
Outboard end (0.405 semispan)	2.81
Sweepback of the hinge line, deg	27.8
Total flap area added by flap trailing-edge extension sq ft	6.68
Horizontal tail	
Total area, including blanketed areas, sq ft	98.9
Span, ft	18.7
Aspect ratio	3.54
Taper ratio	0.30
Mean aerodynamic chord, ft	5.82
Sweepback of the quarter-chord line, deg	45
Dihedral angle, deg	0
Tail length, $\bar{c}/4$ to $\bar{c}_t/4$, ft	14.53
Volume, $\frac{S(\text{tail})}{S(\text{wing})} \times \frac{\text{tail length}}{\bar{c}}$	0.33
Fuselage	
Length, ft	48.0
Maximum diameter, ft	6.50
Total inlet area, minimum, sq ft	4.83
Base area, sq ft, approx	10.0
Total tailpipe area, sq ft	4.37

TABLE II.- CONFIGURATIONS TESTED

Flap deflection, deg			BLC		Horizontal tail	Figure no.
δ_f	δ_{N_i}	δ_{N_o}	C_{μ_f}	C_{μ_N}		
0	0	0	0	0	On	4(a),5,8
					Off	5
	60	60	0	0	On	4(a)
				0.022	On	4(b),8
45	60	60	0	0.021	On	8
			0.0022	0.021	On	8
			variable	0.021	On	10
55	0	0	0	0	On	4(a)
			0.0025	0	On	4(b),6,8
					Off	8
		60	0.0025	0.017*	On	6
	20	60	0.0024	0.020*	On	6
	40	40	0.0025	0.023	On	6
		60	0.0025	0.015*	On	6
			0.0024	0.018*	On	5,6
					Off	5
			0.0027	0.022	On	6
		70	0.0027	0.037	On	6
			.0026	0.014*	On	6
	60	60	0	0	On	4(a)
			0.0035	0	On	4(b)
			variable	0	On	10
			0.0026	0.020	On	4(b),6,7,8
			0.0025	0.005	On	7
				0.010	On	7
				0.032	On	7
			0.0024	0.014*	On	6
				variable	On	9
				0.080	Off	5
				0.076	On	5,6,7
		60 plus gloves	0.0026	0.040	On	6
				0.028*	On	6,7
				0.017*	On	7
		70	0.0027	0.036	On	6
				0.015*	On	6,7
				0.025*	On	7
	70	70	0.0025	0.081*	On	6
			0.0022	variable	On	9
65	0	0	0.0052	0	Off	8
	60	60	0	0.021	On	8
			0.0052	0.021	On	8
			variable	0.021	On	10

*Leading-edge boundary-layer control applied outboard only (0.4 to 1.0 b/2)

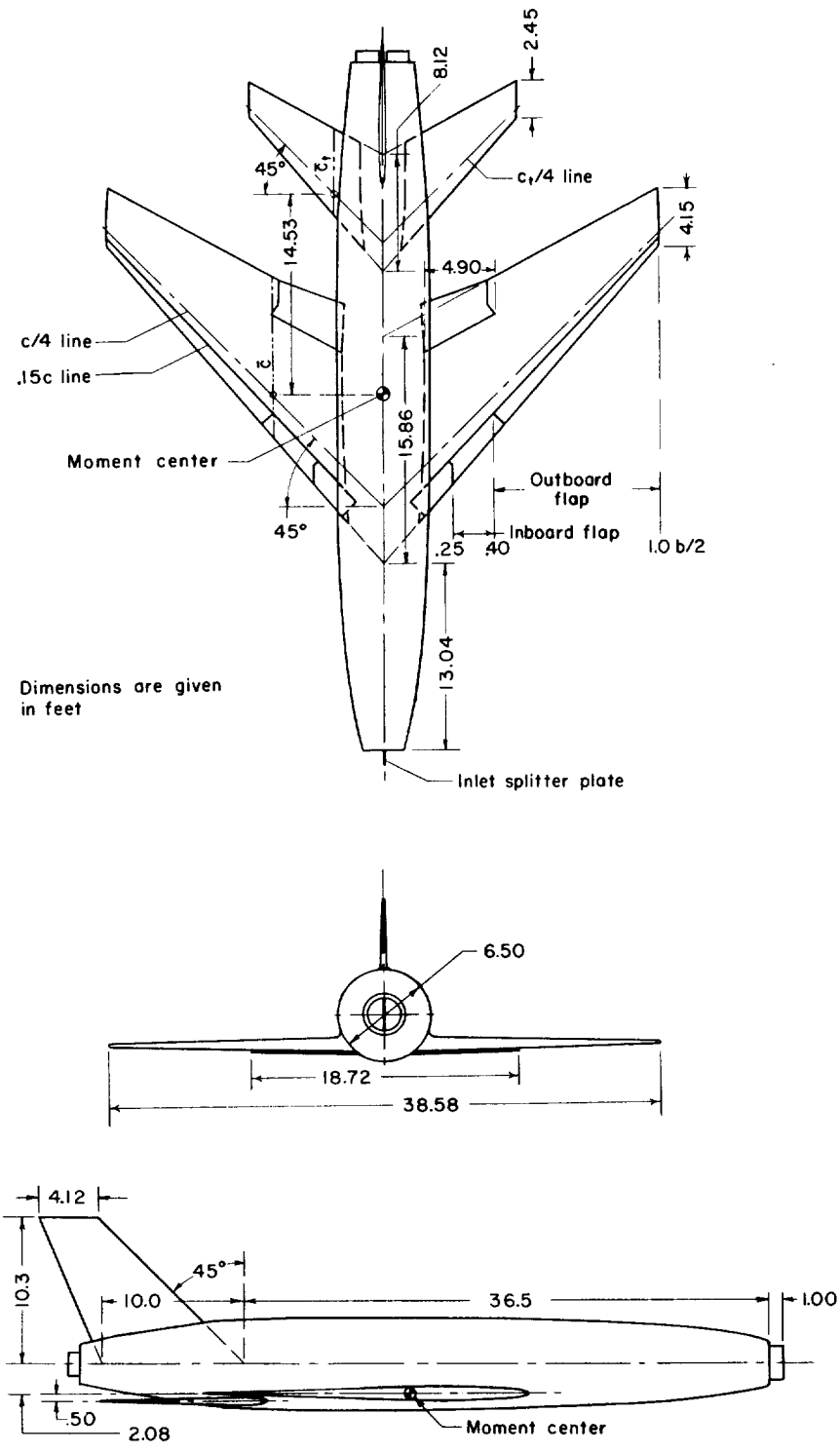

Figure 1.- Three-view sketch of the model.

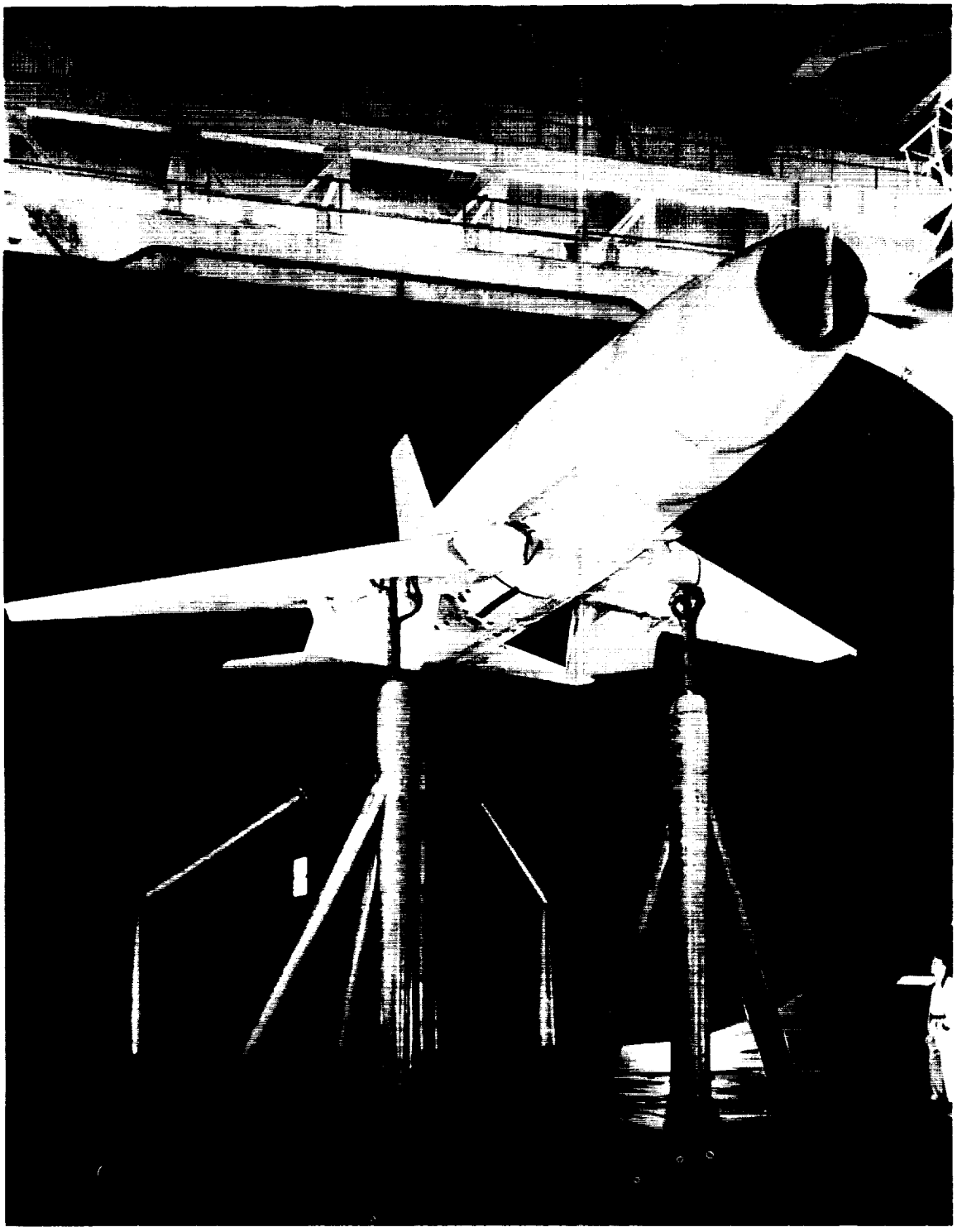

A-22513

Figure 2.- View of the model installed in the wind tunnel.

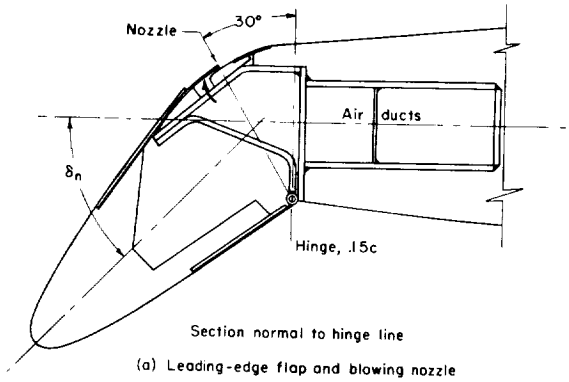

Section normal to hinge line

(a) Leading-edge flap and blowing nozzle

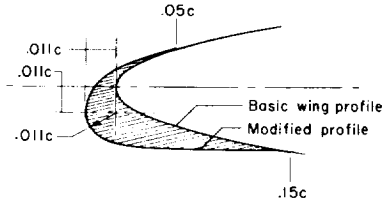

Section normal to leading edge

(b) Leading-edge glove with camber and increased radius

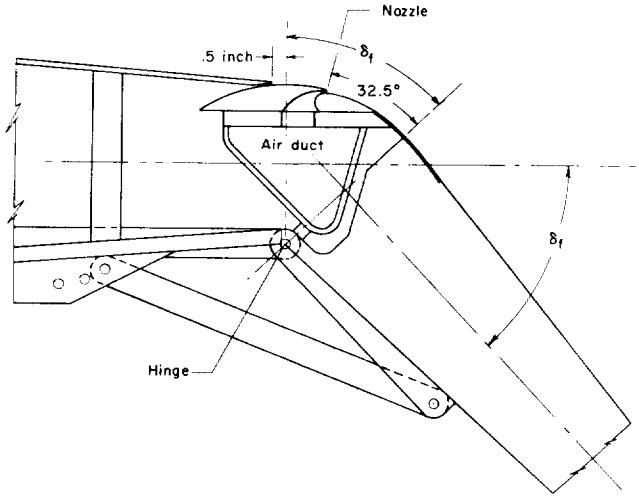

Section normal to hinge line

(c) Trailing-edge flap and blowing nozzle

Figure 3.- Details of wing high-lift devices.

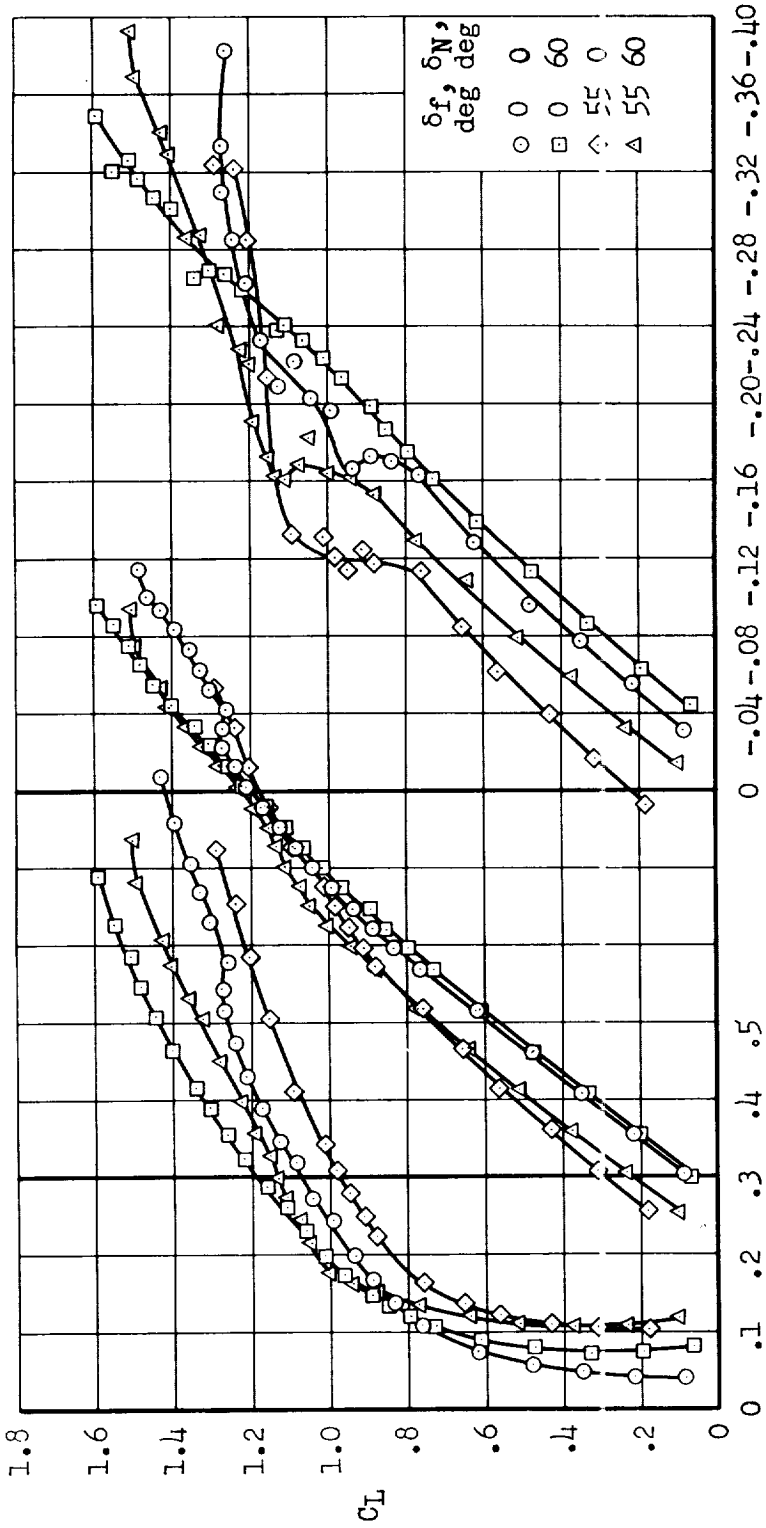

(a) Without boundary-layer control.

Figure 4.- Characteristics of the model with trailing-edge flaps deflected 0° and 55°, and leading-edge flaps deflected 0° and 60° full span; horizontal tail at 0° incidence.

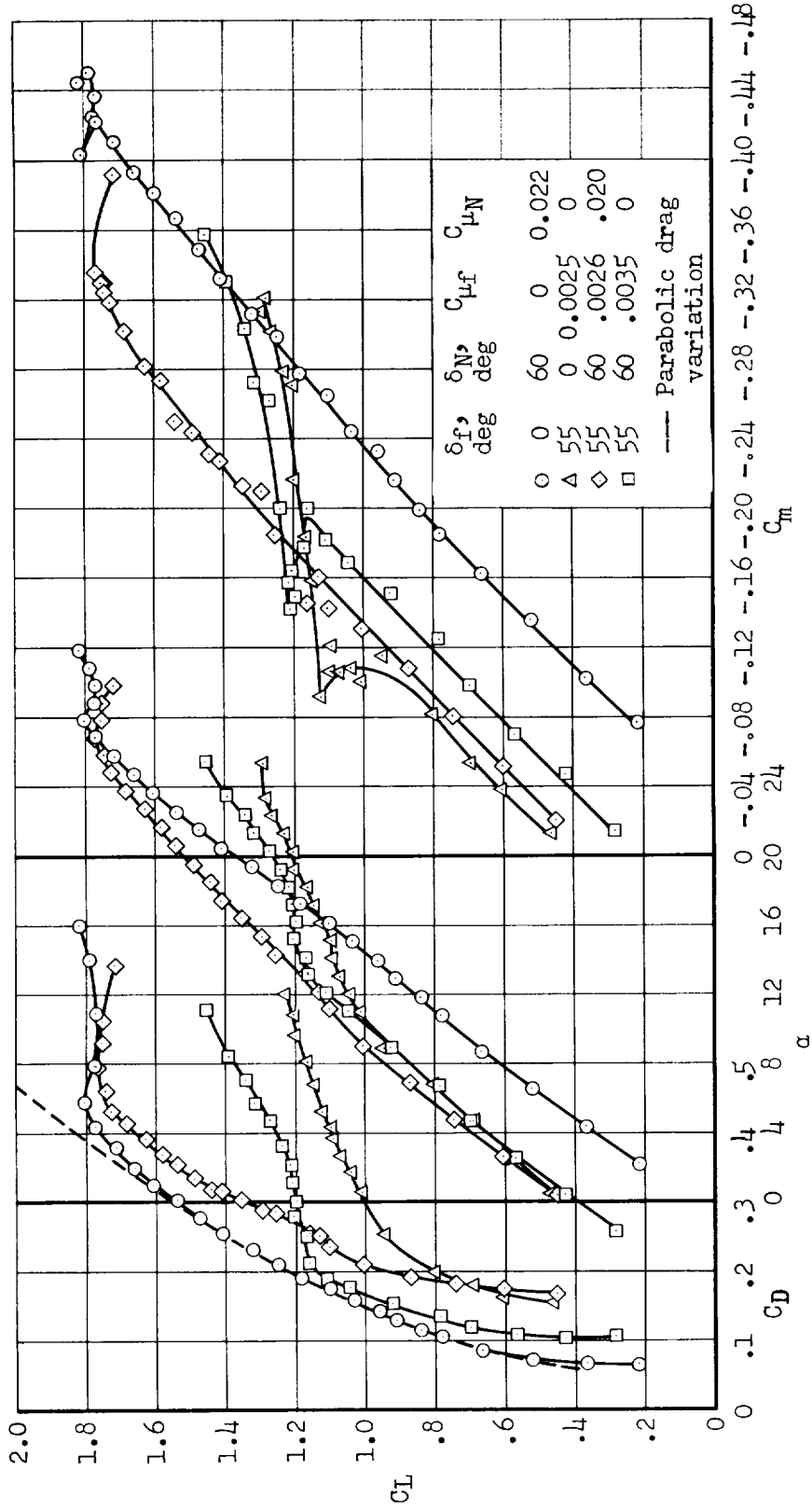

(b) Effects of boundary-layer control.

Figure 4.- Concluded.

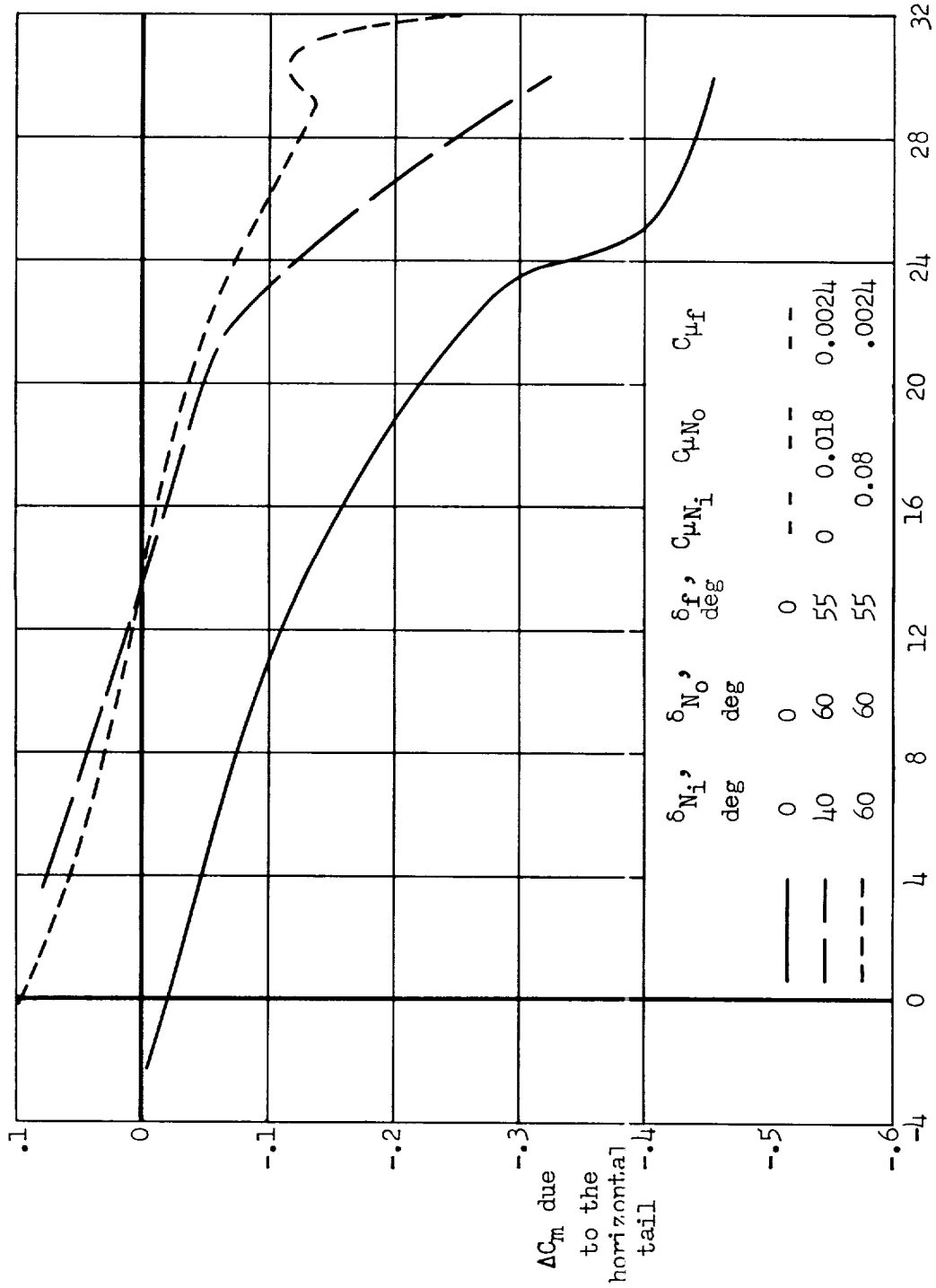

Figure 5.- Effect of the horizontal tail on the pitching-moment characteristics of the model. Tail-on data measured with 0° incidence.

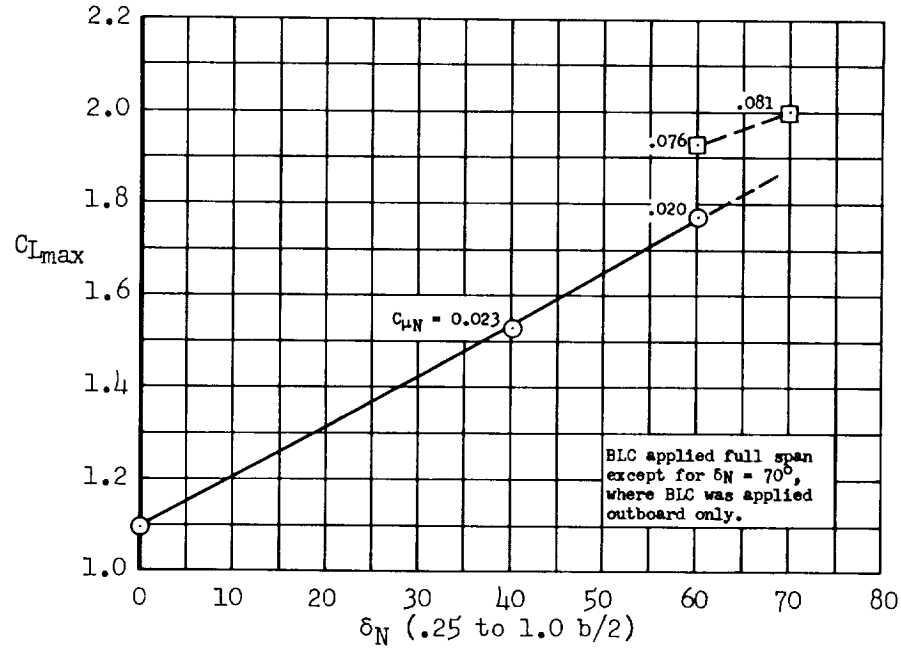

(a) Full-span leading-edge flap deflection.

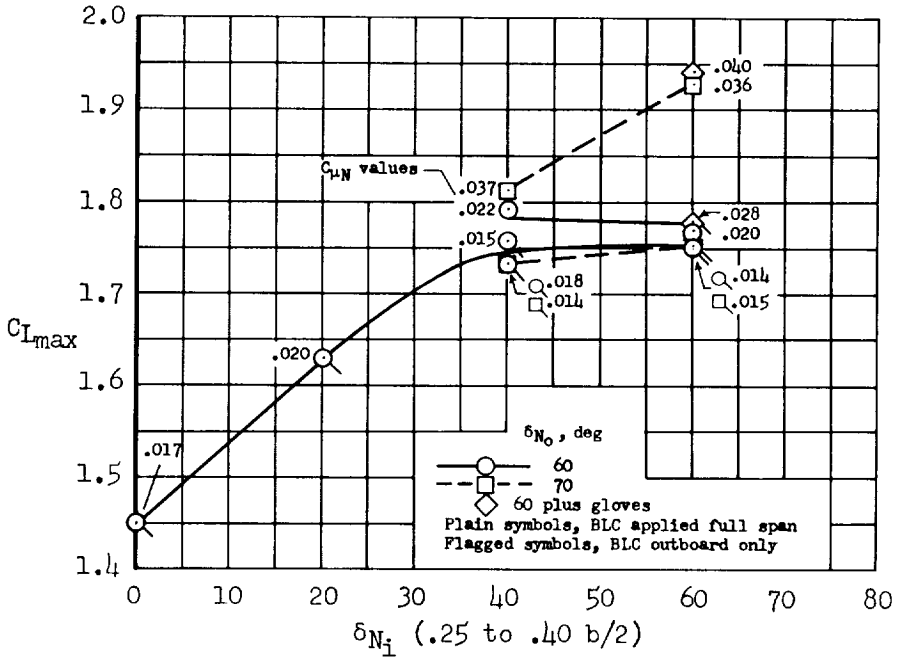

(b) Inboard leading-edge flap deflection and outboard gloves.

Figure 6.- Effects of variations in leading-edge flap deflection and boundary-layer control on the maximum lift of the model with trailing-edge flaps deflected 55°; C_{μ_f} = 0.002; horizontal tail on.

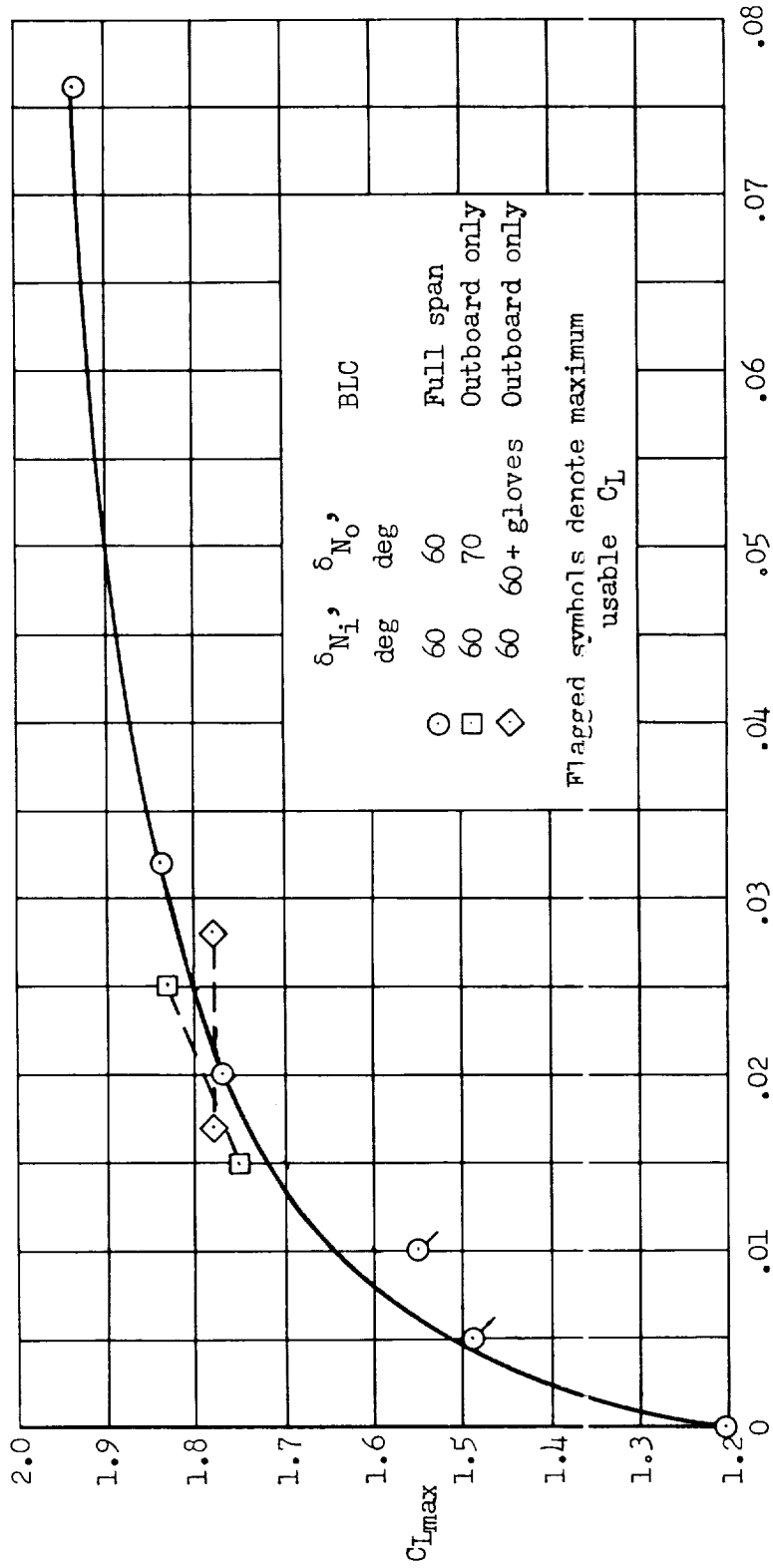

Figure 7.- Effect of changes in C_{μ_N} on the maximum lift of the model with trailing-edge flaps deflected 55°; C_{μ_f} = 0.0025; horizontal tail on.

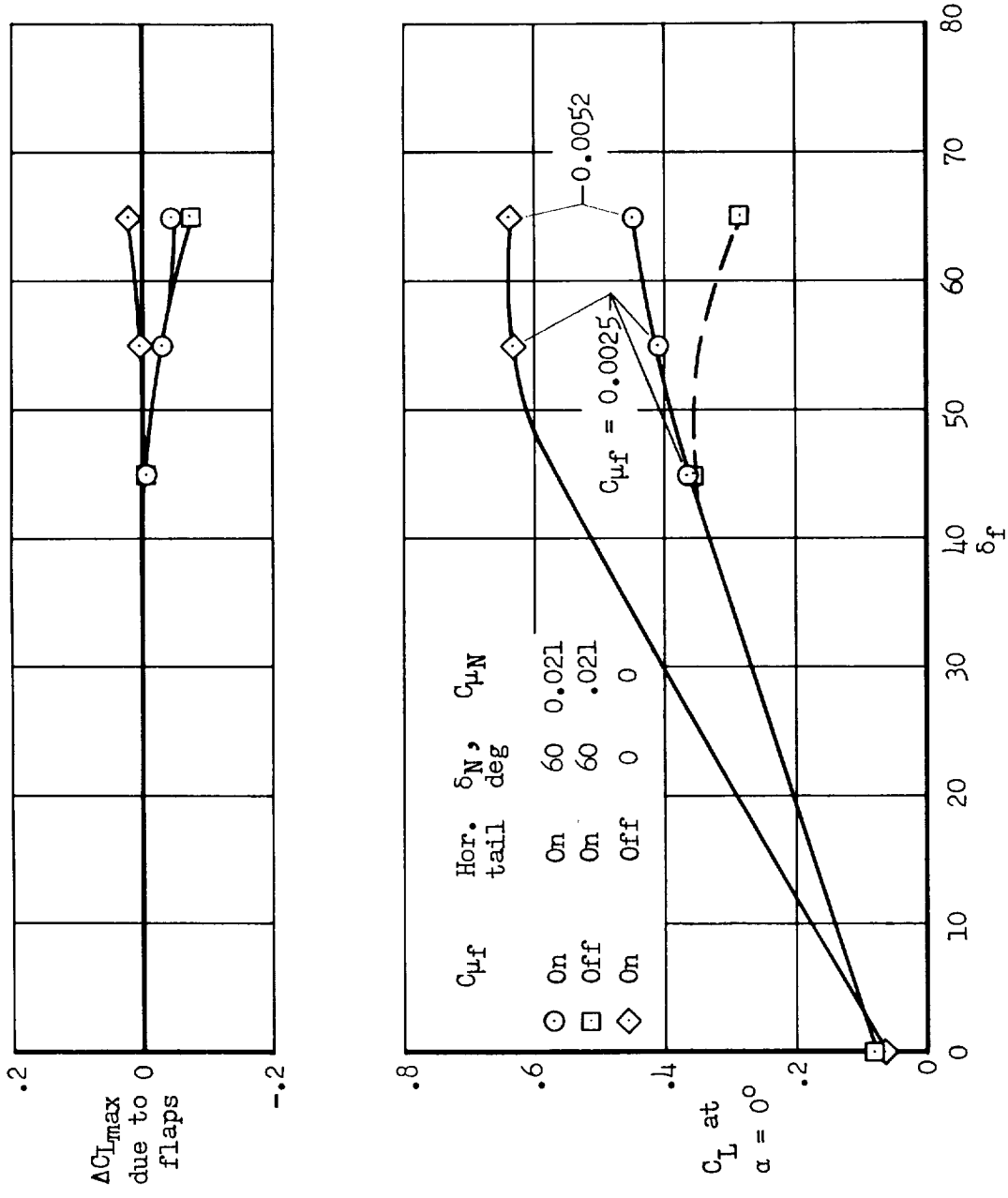

Figure 8.- Effects of trailing-edge flap deflection and boundary-layer control on the lift of the model.

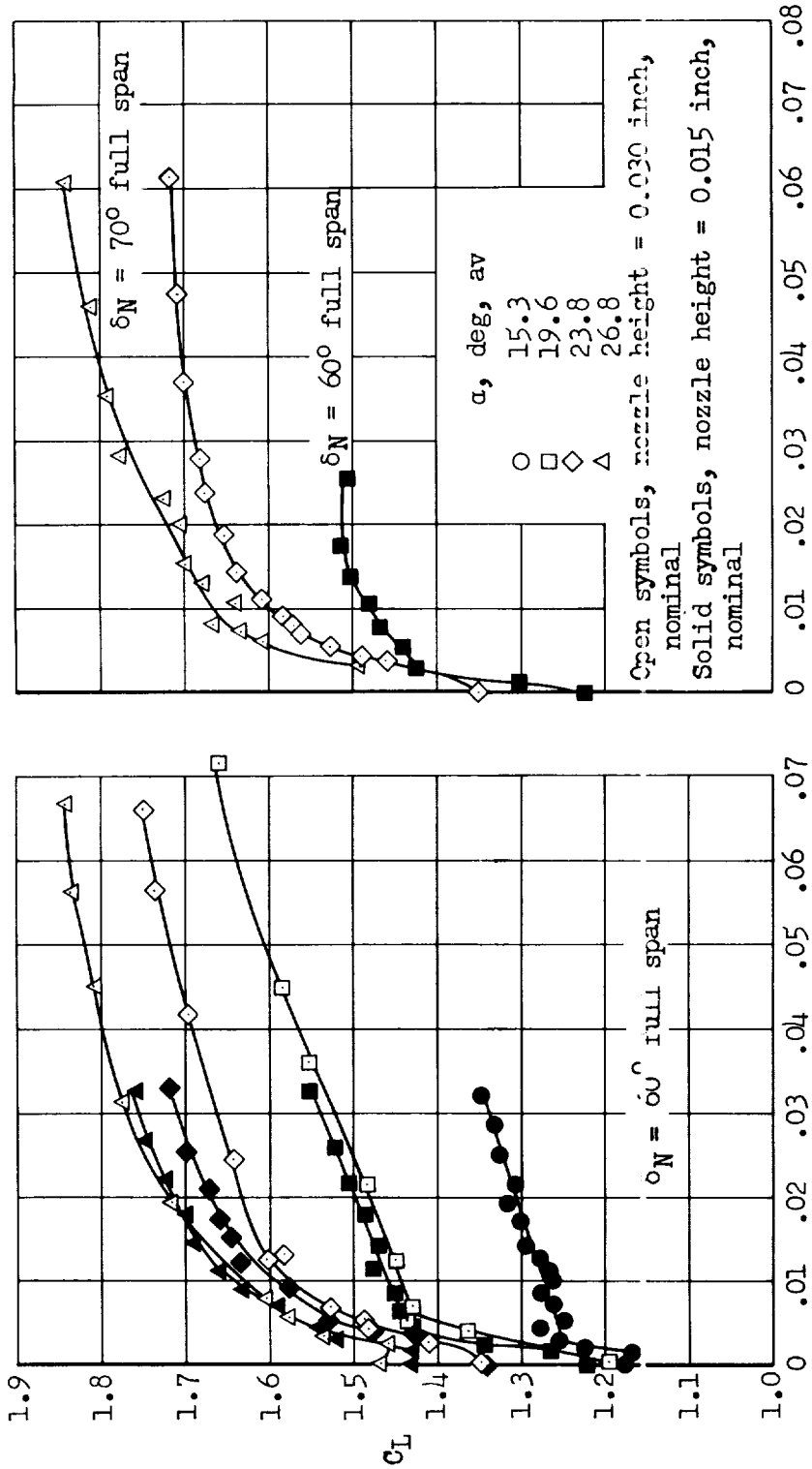

Figure 9.- Variations of lift coefficient with leading-edge flap flow coefficient at several angles of attack; trailing-edge flaps deflected 55°; $C_{\mu f}$ = 0.0024; horizontal tail on.

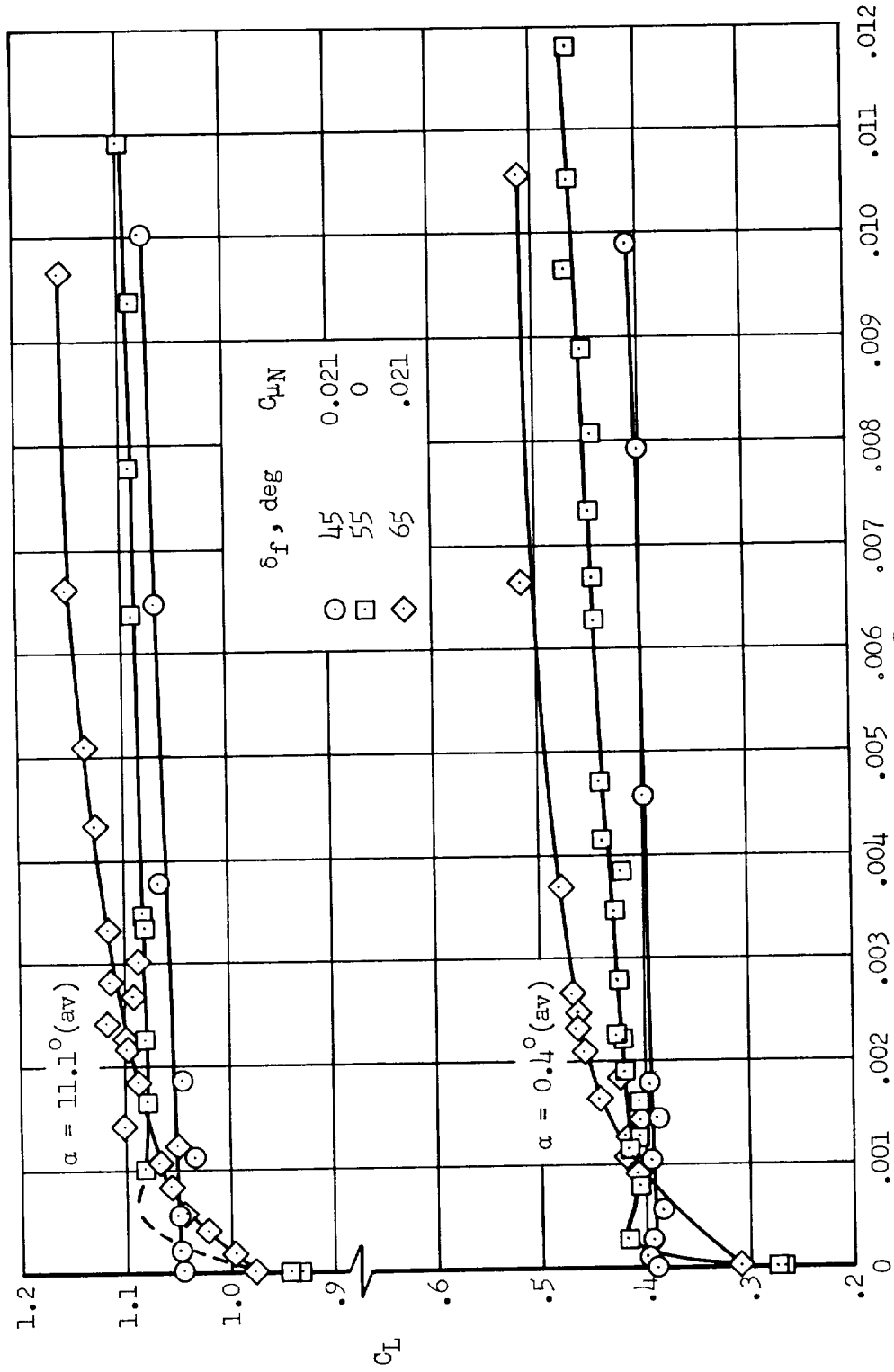

Figure 10.- Variations of lift coefficient with trailing-edge flap flow coefficient for several flap deflections; leading-edge flaps deflected 60° full span; horizontal tail on.